

# Large-scale weather patterns favorable for volcanic smog occurrences on O'ahu, Hawai'i

Kristine Tofte<sup>1</sup> · Pao-Shin Chu<sup>1</sup> · Gary M. Barnes<sup>1</sup>

Received: 2 April 2017 / Accepted: 6 August 2017  
© Springer Science+Business Media B.V. 2017

**Abstract** Kīlauea Volcano, located on the Island of Hawai'i, released approximately 3700 t of sulfur dioxide (SO<sub>2</sub>) per day from April 2009 through 2014. Within the atmosphere, SO<sub>2</sub> is oxidized and converted to sulfuric-acid aerosols, and this volcanic smog is commonly referred to as vog. This study focuses on large-scale weather patterns that bring vog to O'ahu. The Hawai'i State Department of Health PM<sub>2.5</sub> measurements were used to identify elevated vog conditions, and a total of 101 vog days were found. European Centre for Medium-Range Weather Forecasts ERA-Interim reanalysis data were used to determine weather patterns. These 101 vog days were the result of 57 distinct vog events lasting from 3 h up to 4 days. The 57 events were further categorized into three large-scale weather patterns: pre-cold fronts (37 cases), upper-level disturbances (17 cases), and Kona lows (3 cases). The pre-cold front events had variable duration lasting up to 4 days, and the largest vog concentrations occurred during long-duration pre-cold front events. Trade winds did not transport vog to O'ahu. As part of this effort, ERA-Interim data were downscaled to a resolution of 10 km and then 3.3 km using the Weather Research and Forecasting (WRF) model. The downscaled reanalysis data were used as input by the Hybrid Single-Particle Lagrangian Integrated Trajectory (HYSPLIT) model. The HYSPLIT model allowed for a visual representation of how vog is advected by large-scale wind patterns.

**Keywords** Atmospheric science · Synoptic patterns · Air quality · Pollution · Volcanic smog · Volcanic activity · Health

## Introduction

The Hawaiian archipelago should have some of the cleanest air in the world because of its location in the mid-ocean. However, the air quality is occasionally poor because of volcanic smog (vog) emanating from Kīlauea Volcano which is located on the southeast corner of the Island of Hawai'i, also known as the Big Island (Fig. 1).

Kīlauea Volcano started erupting continuously in 1983, mainly from the Pu u Ō ō vent located on the East Rift Zone. In March 2008, an additional vent opened in the Halema uma u crater at the volcano's summit. The gases emitted from the two vents comprise primarily of water vapor (H<sub>2</sub>O), carbon dioxide (CO<sub>2</sub>), and sulfur dioxide (SO<sub>2</sub>), along with other minor trace gases. The main gas of interest being released from the vents is SO<sub>2</sub>. During the time from January 2009 to January 2015, the two vents released an average of 3700 ± 1400 t of SO<sub>2</sub> every day (J. Sutton, United States Geology Survey (USGS), Hawaiian Volcano Observatory (HVO), personal communication).

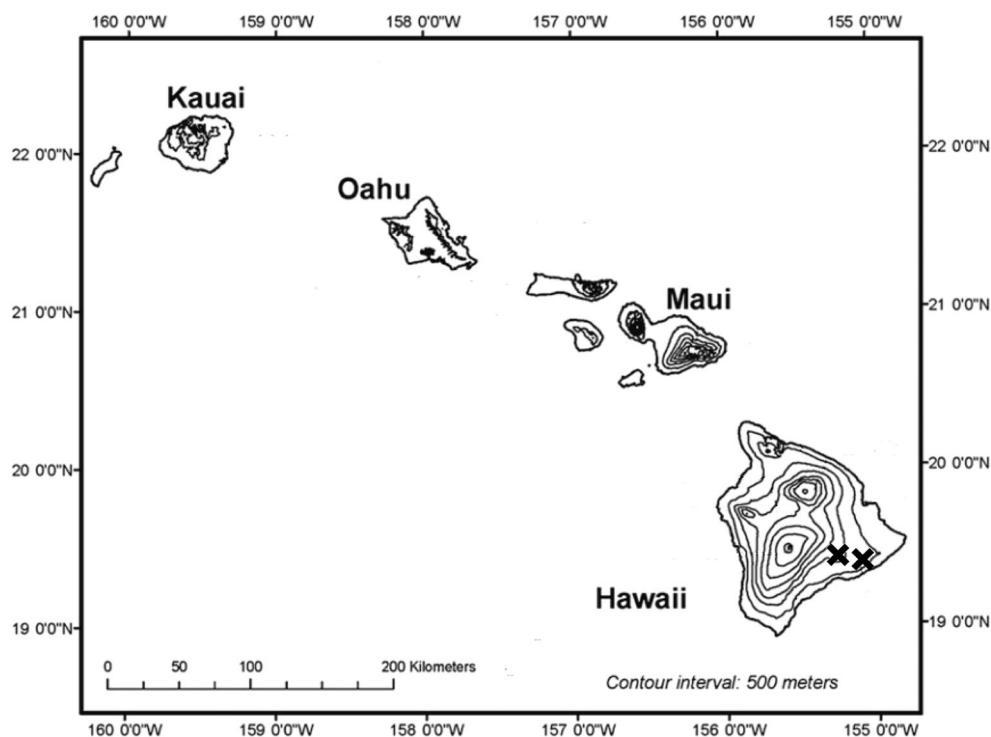
The subtropical high pressure located to the north or north-east of the Hawaiian Islands, depending on the time of year, generate trade winds that are present about 90% of the time in summer and about 65% of the time in winter (Garza et al. 2012). During trade wind conditions, the plume from the active volcano is carried offshore and along the Kona Coast, which is on the west side of the Big Island. When the winds become light and variable, or from the south, the volcanic plume can affect the air quality almost anywhere in the archipelago. Regardless of the wind direction, SO<sub>2</sub> is a problem near Kīlauea's active vents because the SO<sub>2</sub> oxidation half-life

---

✉ Kristine Tofte  
kristine\_tofte@hotmail.com

<sup>1</sup> Department of Atmospheric Sciences, University of Hawai'i at Mānoa, 2525 Correa Rd, HIG 318, Honolulu, HI 98622, USA

**Fig. 1** Map showing the main Hawaiian Islands and their elevation. The two crosses represent the two vents, Halema'uma'u (left) and Pu'u'Ō'ō (right)



is estimated to be about  $6 \pm 4$  h (Porter et al. 2002). During this time, the gaseous  $\text{SO}_2$  in the atmosphere will react with sunlight, dust, and moisture to create sulfuric aerosols ( $\text{SO}_4$ ). Therefore, vog consists of mainly gaseous  $\text{SO}_2$  near the vents and mainly particulate  $\text{SO}_4$  farther away. The particulate  $\text{SO}_4$  can consist of sulfuric acid ( $\text{H}_2\text{SO}_4$ ), ammonium sulfate ( $(\text{NH}_4)_2\text{SO}_4$ ), and/or ammonium bisulfate ( $(\text{NH}_4)\text{HSO}_4$ ), where the first one is very acidic, the second is less acidic, and the last one is partially neutralized (John Porter, University of Hawai'i at Mānoa, personal communication).

When  $\text{SO}_2$  is inhaled, many individuals experience a dry cough and hay fever symptoms. The highly acidic  $\text{SO}_4$ , on the other hand, will give individuals sinus congestion and bronchitis-like symptoms (Longo 2009).  $\text{SO}_4$  can irritate the lungs and the mucus membranes. This has a negative effect on the efficiency of respiration and also compromises the immune system. Another adverse health outcome can include premature mortality (Fann and Risley 2013, Li et al. 2016). Children, those with chronic asthma or other respiratory impairments, and individuals with circulatory problems are especially vulnerable to  $\text{SO}_4$ . Symptoms may include breathing difficulties, coughing, sore throat, flu-like symptoms, headaches, eye irritation, lack of energy, and more mucus production (Durand and Grattan 2001; Longo 2013).  $\text{SO}_4$  can also make rainfall acidic, which affects various crops and nursery industries, forests, and lakes. Acid rain can leach lead from rainwater catchment systems into the water supply. In

addition, dense vog can reduce visibility and create a potential hazard for drivers, as well as for marine and aviation interests (Sutton et al. 2000).

The Hawai'i State Department of Health (DOH) monitors  $\text{SO}_4$  under the category of particulate matter smaller than  $2.5 \mu\text{m}$  ( $\text{PM}_{2.5}$ ). The unit for  $\text{PM}_{2.5}$  is micrograms per cubic meter of air ( $\mu\text{g}/\text{m}^3$ ). The other type of particulate matter is  $\text{PM}_{10}$ , which has a size of  $2.5\text{--}10 \mu\text{m}$ . The Air Quality Index (AQI) is used as a proxy for the associated health effects, and the Environmental Protection Agency (EPA) has calculated the AQI for five major air pollutants: ozone, carbon monoxide, sulfur dioxide, nitrogen dioxide, and particulate matter. The air quality is satisfactory for particulate matter or  $\text{PM}_{2.5}$  when the AQI is between 0 and 50 ( $0\text{--}12 \mu\text{g}/\text{m}^3$ ). At these low values,  $\text{PM}_{2.5}$  poses little or no risk. When the AQI is between 51 and 100 ( $12.1\text{--}35.4 \mu\text{g}/\text{m}^3$ ), the air quality is moderate; this means that people with respiratory issues may need to take precautions.

The EPA has both state and federal ambient air quality standards for  $\text{PM}_{2.5}$ , where the federal primary standard states that the 24-h average should not exceed  $35 \mu\text{g}/\text{m}^3$  and the annual average should not exceed  $12 \mu\text{g}/\text{m}^3$ . However, there are currently no standards made specifically for the State of Hawai'i. Hawai'i is unique compared to the rest of the country, because it has an active volcano surrounded by ocean. During summertime, sea salt from ocean spray ejected into the air by strong trade winds can cause background pollutions for the  $\text{PM}_{2.5}$  measurements.

The goal of this study is to identify the large-scale weather patterns that cause vog to reach the island of O'ahu. O'ahu is chosen because about one million people live on the island. We used PM<sub>2.5</sub> data at one site, one reanalysis dataset, ocean analysis charts, and the Weather Research and Forecasting (WRF) model and the Hybrid Single-Particle Lagrangian Integrated Trajectory (HYSPLIT) model to address the following questions: (1) When do vog events occur on O'ahu? (2) How frequent are vog events? (3) What levels of vog does O'ahu usually experience? (4) What is the typical duration of a vog event? (5) What types of large-scale weather patterns are associated with vog events? This will allow more information to the general public and also be a useful tool in forecasting vog events.

The paper is organized as follows: the “Data and models” and “Methodology” sections describe the datasets, models, and methods used in this study, respectively; the “Description of main weather categories” section covers the description of main weather categories; results are presented in the “Results” section; this is followed by a summary and discussion in “Conclusion and Discussion” section.

## Data and models

### DOH data

The Clean Air Branch of DOH monitors the ambient air in the State of Hawai'i (State of Hawai'i Department of Health 2014). The main pollutant of interest is PM<sub>2.5</sub>, which is recorded by four stations on O'ahu including Kapolei, Pearl City, Sand Island, and Honolulu. However, due to background pollution from industrial areas and power plants for the first three sites, only measurements at Honolulu are used. These are taken at the roof of the DOH building in downtown Honolulu, at 21.31°N and 157.86°W (~ 350 km away from the vents). This station monitored PM<sub>2.5</sub> from April 2009 to 2014. There was a total of 3498 missing hours from the study period, equivalent to approximately 7% of the study period. The years with the most missing data were 2013 and 2014. The PM<sub>2.5</sub> measurements are taken using the beta-attenuation particulate monitor BAM-1020, which automatically measures and records airborne particulate concentration levels using the industry-proven principle of beta ray attenuation.

### ERA-interim data

The ECMWF ERA-Interim initial and boundary conditions are used to drive WRF, which is then used to drive HYSPLIT. The dataset starts on 1 January 1979 and continues to be extended forward in near-real time (Dee et al. 2011). The reanalysis system uses a spectral model

integrated at a T225 (80 km) horizontal resolution with 60 vertical hybrid levels. A four-dimensional variational data assimilation system with 12-h cycling is applied with output every 6 h (Hodges et al. 2011). The period used in this study was from April 2009 through 2014, consistent with the observed PM<sub>2.5</sub> data. Geopotential heights at different levels were used to identify the different large-scale patterns that caused vog to reach O'ahu. The ERA-Interim data are available through <http://www.ecmwf.int/en/research/climate-reanalysis/era-interim>.

### NOAA ocean analysis

The National Oceanic and Atmospheric Administration (NOAA) offers ocean analysis products through the Service Records Retention System (SRRS). The ocean analysis products were independent from the ERA-Interim data and provided more detailed synoptic-scale weather information (not shown). The data were used to verify the ERA-Interim reanalysis data. SRRS stores weather observations, summaries, forecasts, warnings, and advisories provided by the US National Weather Service (NWS). These are available from the NOAA Operational Model Archive and Distribution System (NOMADS): <http://nomads.ncdc.noaa.gov> (Rutledge et al. 2006).

### WRF model

The WRF-ARW model was used to dynamically downscale the ERA-Interim data to 10 km and eventually 3.3 km, which is done to include more local-scale effects when running the HYSPLIT model. The outer domain has a 10-km resolution and covers a 45° by 45° area with the Hawaiian Islands in the middle. The inner domain has a resolution of 3.3 km and covers a 20° by 20° with the Hawaiian Islands and surrounding water in the middle. WRF is a mesoscale numerical weather prediction system for atmospheric research (Skamarock et al. 2008). The model is computationally efficient, and its two-way nesting capabilities allow fine grid resolution. The simulations in WRF had 38 levels in the vertical and four soil layers. The physics scheme used for cloud microphysics was the WRF Single-Moment 3-class, which is a simple and efficient scheme with ice and snow processes suitable for meso-scale grid sizes. The Rapid Radiative Transfer Model was used as a physics scheme for the longwave radiation. Dudhia, which has simple downward integration allowing efficient cloud and clear-sky absorption and scattering, was used for the shortwave radiation physics scheme. The Yonsei University scheme was used for the boundary layer physics. This is a non-local-K scheme with explicit entrainment layer and parabolic K profile in the unstable mixed layer. The Noah Land Surface Model scheme: Unified NCEP/NCAR/AFWA scheme, which includes soil temperature and moisture in four

layers, fractional snow and frozen soil physics, was used for the land surface processes. The Tiedtke scheme was used for the cumulus convection. This mass-flux scheme has CAPE-removal time scale, shallow component and momentum transport.

### The HYSPLIT model

The Hybrid Single-Particle Lagrangian Integrated Trajectory (HYSPLIT) model was developed by NOAA Air Resources Laboratory (ARL) (Draxler and Hess 1998). HYSPLIT is one of the most widely used models for atmospheric trajectory and dispersion calculations (Fleming et al. 2012). The model can compute trajectories, ensemble trajectories, complex dispersion, and deposition simulations. HYSPLIT is also used by the Vog Measurement and Prediction (VMAP) project that monitors the emissions from Kīlauea volcano and has developed a numerical forecast of vog dispersion available to the public (Businger et al. 2015).

### Methodology

The DOH hourly  $PM_{2.5}$  data were used to find vog days. A day was classified as voggy if there were at least three consecutive hours of  $PM_{2.5}$  greater than or equal to  $13 \mu\text{g}/\text{m}^3$ . The threshold of  $13 \mu\text{g}/\text{m}^3$  was set to be beyond the “satisfactory” level according to the AQI for particulate matter as described in the “Data and models” section. When the air quality has the value of  $13 \mu\text{g}/\text{m}^3$ , it is considered moderate. A total of 101 vog days from April 2009 to 2014 for station Honolulu were identified.

In the second step, the 101 vog days were analyzed using ERA-Interim’s Mean Sea-Level (MSL) pressure, and the 850-, 500-, and 250-geopotential heights along with the ocean analysis data to determine the preferred synoptic patterns associated with vog days. When studying the synoptic settings along with elevated hourly  $PM_{2.5}$ , the analysis showed that the 101 vog days are actually a part of 57 events with varying duration from 1 to 4 days. Examination of the 57 vog events showed that they were associated with three weather categories: pre-cold fronts, Kona lows, and upper-level disturbances, described in more detail in the “Description of main weather categories” section. For the pre-cold fronts, there are two subcategories depending on the duration of the vog episode. Long-duration events are those that lasted longer than 1 day, and those lasting only 1 day are considered short duration.

In the third step, the WRF model was used to dynamically downscale the ERA-Interim reanalysis data for each case study. The reanalysis data had a resolution of 80 km and was downscaled to a horizontal resolution of first the 10 km and then 3.3 km to include local-scale circulations.

Specifically, the four case studies included two pre-cold fronts of short and long duration, one Kona low and one upper-level disturbance. The four case studies were chosen to be representative from a larger set of runs. We initially looked at the synoptic patterns for each of the four types and selected a subset to identify basic features. Strong similarities were found in the subset of runs, but only four were presented due to space considerations.

WRF was initialized 2 days prior to the vog event to allow the model to spin up and include the large-scale synoptic patterns before the vog plume reached O’ahu. Each WRF simulation took about 10 h to run depending on how long the vog event lasted. Another reason for choosing only four case studies was because running the WRF model with a high resolution is computationally expensive.

For the last step, the WRF output was used in the HYSPLIT model to create ensemble trajectory and concentration plots for each of the four case studies. The ensemble trajectory starts multiple trajectories from the original start location. Each trajectory is calculated by offsetting the meteorological data by a fixed grid factor, which is one grid point in the horizontal and 0.01 sigma units in the vertical. The total is 27 trajectories for all possible offsets in the x, y, and z direction, which can be displayed in any order as red, blue, and green (Draxler and Hess 1998). Yellow has a high concentration, and light blue will have the lowest concentration. The Halema uma u vent is located 1247 m above mean sea level (msl) with coordinates (19.41°N, 155.29°W), and the Pu u Ō ō vent is 698 m above msl with coordinates (19.39°N, 155.11°W). The plume height is assumed to be 500 m above the ground. The gaseous  $SO_2$  was converted immediately to particulate  $SO_4$  after being released. Wet and dry depositions were included in the calculations to represent a more viable deposition mechanism for the vog particles. The emission rate from the two vents was set to release the average value of 150 t of  $SO_2$  per hour continuously, which is based on the daily average of 3700 t.

The start time for each case study in HYSPLIT varied depending on event type due to varying wind strength and wind direction. The 1-day cold front was initialized 31 January 2010 at 1200 UTC (0200 HST, Hawaiian Standard Time) 2 days prior to the event, and the 4-day cold front was initialized on 21 January 2010 at 1800 UTC (0800 HST) 1 day prior to the event. The Kona low and upper-level disturbance events were both initialized at 1200 UTC (0200 HST) 1 day prior to the event 1 May 2010 and 21 May 2013, respectively.

The vog plume’s travel time from the Big Island to O’ahu varies according to wind strength and direction. The straight-line distance from the vents to Honolulu is about 350 km. A typical wind speed between 4 and 10 m/s would give the vog plume 10 to 24 h to reach

Honolulu. Accordingly, all case studies were simulated for a minimum of 72 h.

## Description of main weather categories

### Pre-cold fronts

In winter, the trade winds over the Central North Pacific are frequently disrupted by the passage of mid-latitude cold fronts that penetrate into the subtropics. Most cold fronts dissipate or pass to the north of the Hawaiian Islands, because of the modification of the cooler air mass by the underlying warm ocean as it approaches Hawai'i. The mean number of frontal passages at Kauai per winter is about 16, but only about 9 frontal passages will make it farther southeast to the Big Island (Worthley 1967).

In this study, a cold front was defined when (1) a low-pressure system with its associated frontal boundary approaches the islands, and (2) the subtropical high is pushed further to the east. Vog is brought to O'ahu before the cold front has passed the islands, while winds have a southerly component. Hence, the cold front category will be referred to as pre-frontal. After the frontal passage, winds turn to northerly and/or northwesterly. This wind shift can bring back some additional concentrations of vog.

An important feature about the pre-cold front events is the duration. Some events only lasted a couple of hours while other events could go on for several days. Stronger cold fronts usually move through the island chain much faster than the weaker cold fronts or shear lines. The longer-duration events could also have a stalled front that dissipated before even reaching O'ahu, and the events were also longer if there were multiple fronts involved. Thirty-seven pre-cold fronts were found in this study, which included 18 cold front events lasting more than 1 day and 19 cold front events lasting less than 1 day. The 18 long-duration pre-cold front events had a mean and median value of  $18 \mu\text{g}/\text{m}^3$ . The 19 short-duration pre-cold front events had a mean value of  $16 \mu\text{g}/\text{m}^3$  and a median value of  $15 \mu\text{g}/\text{m}^3$ . The highest event value found for the long-duration pre-cold front was  $22 \mu\text{g}/\text{m}^3$ , and the lowest was  $14 \mu\text{g}/\text{m}^3$ . The highest event value found for the short-duration pre-cold front was  $19 \mu\text{g}/\text{m}^3$  and the lowest was  $13 \mu\text{g}/\text{m}^3$ .

### Kona lows

The second type of synoptic pattern that brings vog to O'ahu is a Kona low, also known as a subtropical cyclone. The word *Kona* is Hawaiian and translates to leeward. During Kona low events, the winds shift to a southerly component instead of normal northeast or east. A Kona low, originally identified by Simpson 1952, can last for days without weakening and may

be associated with heavy rains, hailstorms, flash floods, landslides, high winds, large surf, waterspouts, and thunderstorms according to Kodama and Barnes (1997), Morrison and Businger (2000), Otkin and Martin (2004), and Tu and Chen (2011). They are cold core systems with the strongest circulation in the middle and upper troposphere and are usually cut-off from the upper-level subtropical westerlies. A schematic model of a Kona Low is illustrated in Chu et al. (1993).

A Kona low in this study is defined as in Caruso and Businger (2006) and O'Connor et al. (2015) with minor changes: (1) the upper-level low must remain cut off from the mid-latitude westerlies for at least 24 h, (2) the upper-level low's center must pass south of  $35^\circ\text{N}$ , and (3) the low must occur during the cool season which we define as October through May. Three Kona lows were identified as contributors to the vog days. The mean and median values for these three events were both  $17 \mu\text{g}/\text{m}^3$ . The highest event value found was  $17 \mu\text{g}/\text{m}^3$  and the lowest was  $16 \mu\text{g}/\text{m}^3$ . The location of the Kona low was to the north of the Islands, and the duration of the vog event varied from 1 to 2 days.

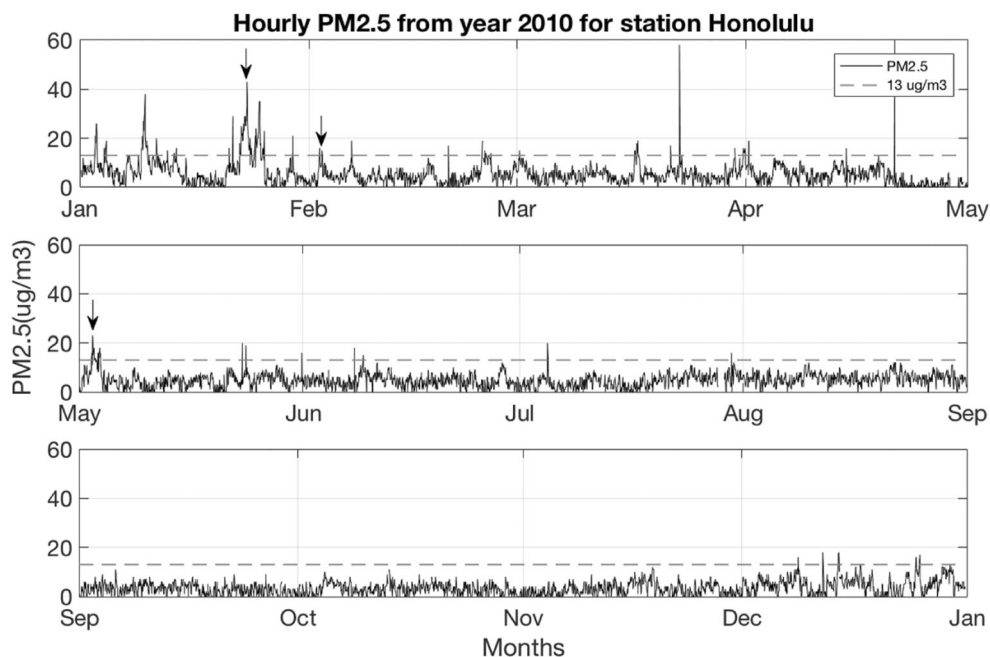
### Upper-level disturbances

The upper-level disturbance pattern can occur any time of year. They have the strongest circulation in the upper troposphere, and when the circulation penetrates downward, this can affect the winds at the surface. Especially, if an upper-level low breaks off from the westerlies, it can penetrate downwards and force the development, or enhance, surface troughs and tropical waves to their east. Under special circumstances, they can induce thunderstorms and contribute to the formation of tropical cyclones. The upper-level disturbance is similar to a Kona low with the downward development. However, a Kona low has a closed circulation at the surface while the upper-level disturbance does not (O'Connor et al. 2015).

One type of upper-level disturbance is the Tropical Upper Tropospheric Trough (TUTT) cell (Sadler 1975). The TUTT cell forms during summer over the ocean and moves west-southwest. These cells have favored ascent and rainfall on their south and east sides, and they have sinking motion on the north and west sides (Kelley and Mock 1982). The TUTT cell has a synoptic scale of about 3000 km in diameter. The TUTT cell is weaker in lower levels, but they can still destabilize the upper atmosphere, eliminate subsidence, and cause heavy rainfall.

In this study, the definition of an upper-level disturbance is fairly simple and includes a trough in the upper levels. There were 17 upper-level disturbances that brought vog to O'ahu during the study period. The mean and median values of  $\text{PM}_{2.5}$  for these 17 events were both  $16 \mu\text{g}/\text{m}^3$ . The highest event value found was  $21 \mu\text{g}/\text{m}^3$  and the lowest was  $14 \mu\text{g}/\text{m}^3$ .

**Fig. 2** Showing hourly PM<sub>2.5</sub> data from station Honolulu for 2010. The dashed line indicates the threshold of 13  $\mu\text{g}/\text{m}^3$ . Arrows indicate events of interest



## Results

### Background climatology

The DOH hourly time series of PM<sub>2.5</sub> for 2010 at station Honolulu was plotted (Fig. 2). The plot shows evidence of an annual cycle with higher values in the winter months than summer months. The PM<sub>2.5</sub> values during summertime never fully reach zero, because the PM<sub>2.5</sub> samples can be contaminated with sea spray. Both the mean and median values of PM<sub>2.5</sub> from Honolulu from April 2009 through December 2014 were 5  $\mu\text{g}/\text{m}^3$ , and the standard deviation

was 5.1  $\mu\text{g}/\text{m}^3$ . These mean and median values fall into the good air quality category.

The annual distribution for the 101 vog days based on Honolulu is shown in Fig. 3. Most of the vog days occurred during winter. January had the highest amount with 20 vog days, and the months June, July, and August had no vog events. May had several vog days and September had only one vog day.

Inter-annual variations in vog days from April 2009 through 2014 are shown in Fig. 4. The years 2012 and 2013 have the highest numbers with 24 and 23 vog days, respectively, and year 2014 has the lowest with 7 vog days. The

**Fig. 3** Vog days per month from station Honolulu for the period from April 2009 through 2014

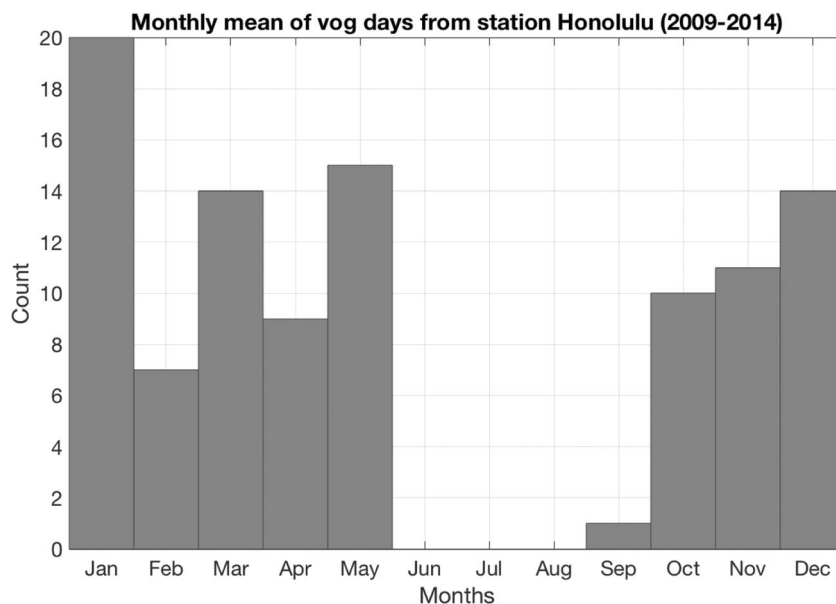
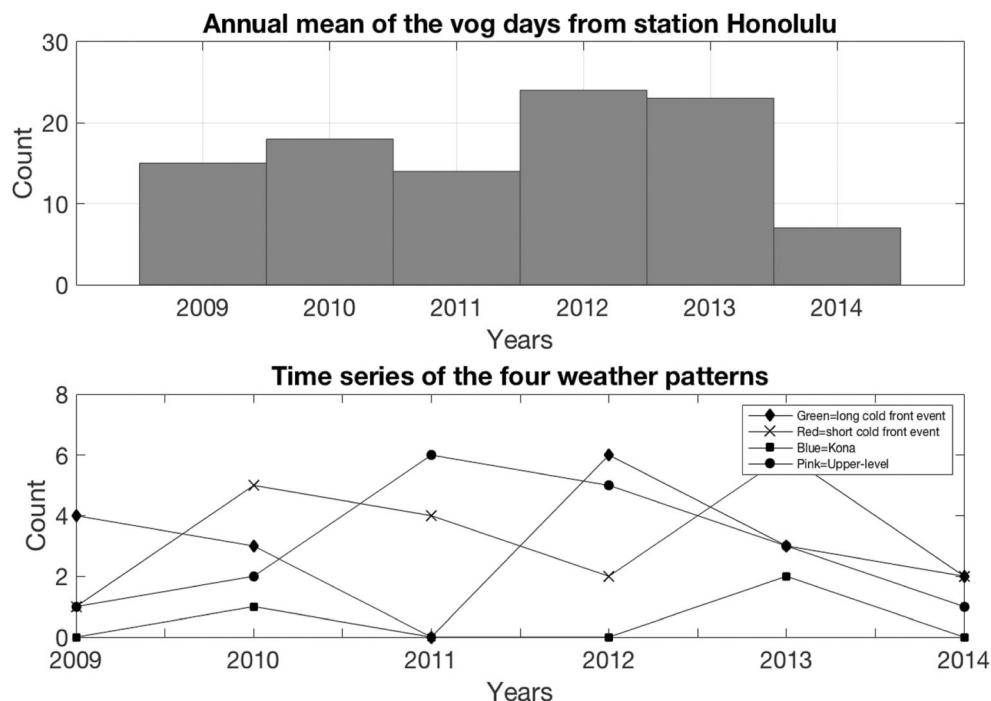


**Fig. 4** Histogram of the annual number of vog days (top) and the annual number of each synoptic pattern (bottom) at station Honolulu



cause of the low value of only 7 vog days in 2014 is unknown, but it could be related to the emission rate from the Kīlauea Volcano, calibration error from the BAM-1020, and/or a change in the large-scale weather patterns unfavorable to bring vog to O'ahu this year. The El Niño Southern Oscillation (ENSO) was also taken into consideration; however, no clear links between vog events and ENSO were found during this short time span (6 years).

On average, Honolulu has approximately 17 vog days per year. The 95% bootstrap confidence interval for this mean is (12.2, 21.2). The bootstrap is a non-parametric, resampling technique for statistical inference, and it operates by generating artificial data batches from the existing sample with replacement (Chu and Wang 1997).

### Case studies

The types of large-scale weather patterns associated with vog events are determined using mainly ERA-Interim reanalysis data, and the ocean analysis charts were used for additional guidance. The ERA-Interim's 6-h output was analyzed 2 days prior to the vog day(s), during the vog day(s), and 1 day after to subjectively determine the type of weather pattern. These episodes fell into three types of synoptic situations: pre-cold fronts, Kona lows, and upper-level disturbances.

#### 1. A short-duration pre-cold front event

The first case study was for a short-duration pre-cold front. The event occurred 2 February 2010, and there were two

peaks in the  $PM_{2.5}$  data that day. One peak is from 0800 to 1100 HST where the values range from 10 to 16  $\mu\text{g}/\text{m}^3$ , and the second peak is from 1600 to 1900 HST where the values are about 10–15  $\mu\text{g}/\text{m}^3$  (Fig. 5a). The ERA-Interim data in Fig. 6 showed clearly where the front was located, while the NOAA Ocean Analysis data showed that the cold front moved through the island chain rather quickly (not shown). The  $PM_{2.5}$  values were high on 2 February because the winds were still southeasterly (Fig. 6a). At 1400 HST 2 February, the cold front was over Kauai, and around 0100 HST the next day, the cold front had passed O'ahu and was located farther east over Maui.

The ERA-Interim reanalysis data for this 1-day cold front event was dynamically downscaled to a resolution of 3.3 km. The data were then run in HYSPLIT to produce an ensemble trajectory plot (Fig. 7a) and concentration plots (Fig. 7b). The ensemble trajectory plot shows the northeast trade winds are first blowing the vog plume to the southwest and out to sea, and a couple of the trajectories get caught in the Big Island wake. The Big Island wake is created mainly by the blocking of the trade-wind layer flow by the high volcanoes that make up the island. This initiates both a clock-wise and an anti-clockwise eddy to the west of the island, shifting the flow towards the western Kona Coast. Vog is usually advected and trapped along the Kona Coast because of strong localized sea breezes. Most of the plume is then blown from the south of the Big Island towards O'ahu and Maui.

After the cold front passed O'ahu, the winds shifted to northwesterly. This brought vog back down the island chain

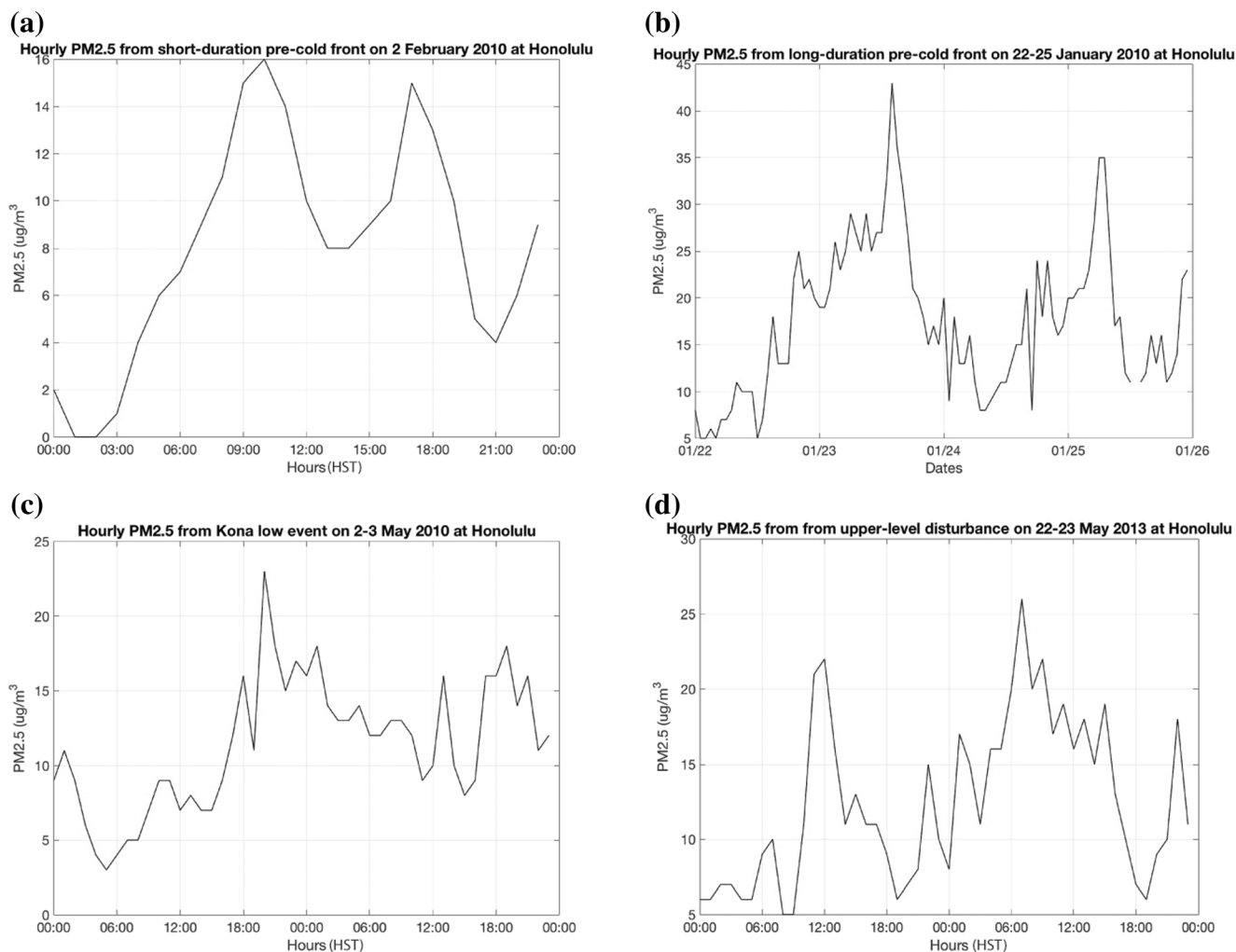


**Fig. 5** Time series of the hourly DOH PM<sub>2.5</sub> data for **a** the short-duration pre-cold front case, **b** the long-duration pre-cold front case, **c** the Kona low case, and **d** the upper-level disturbance case

again, as the subtropical high pressure built back in and the trade winds continued. This pre-cold front wind pattern gave the trajectories a U-shaped path. None of the trajectories traveled above the trade wind inversion which is typically at a 2-km height, and most of them stayed below 1000 m shortly after being released (Fig. 7a, bottom).

The highest concentrations were to the west of the Big Island and Maui and to the northeast of the island chain (Fig. 7b). There was a moderate amount of vog over O'ahu. This figure is consistent with the DOH data, which showed elevated but not too extreme PM<sub>2.5</sub> values. The event mean for the short duration event was 15 µg/m<sup>3</sup>.

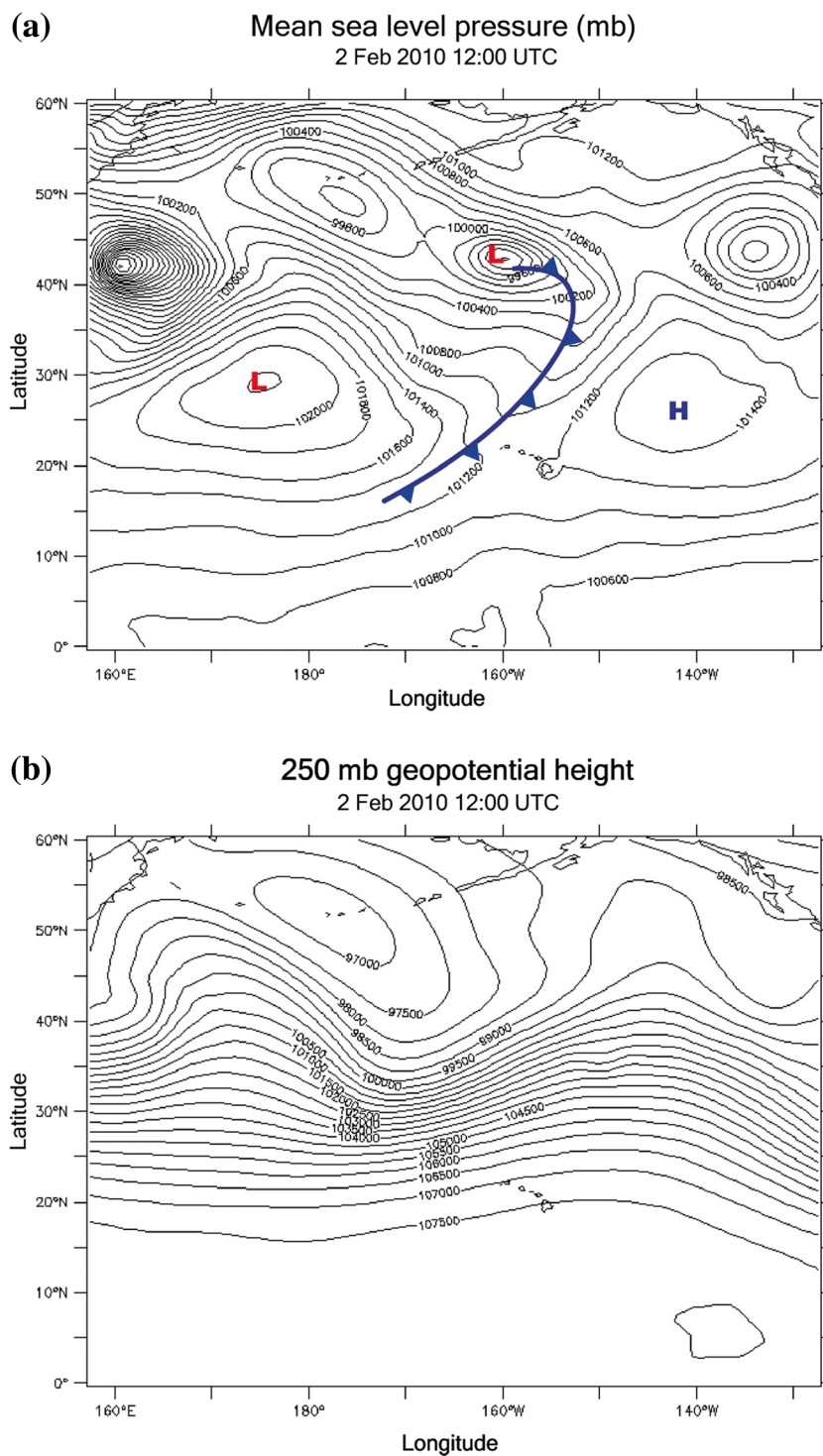
## 2. A long-duration pre-cold front event

The second case study was a long-duration pre-cold front with PM<sub>2.5</sub> values elevated for 4 days. The PM<sub>2.5</sub> started to

increase 0800 HST 22 January 2010 and peaked around 2000 HST with 25 µg/m<sup>3</sup> on the same day (Fig. 9). The next day, the values reach up to 43 µg/m<sup>3</sup> at 1400 HST while slightly lower on 24 January with values ranging from 8 to 24 µg/m<sup>3</sup>, becoming higher again on 25 January with values around 11–35 µg/m<sup>3</sup>. The values decreased on 26 January. This long-duration pre-cold front case study had the highest measured daily PM<sub>2.5</sub> values with the longest duration.

Figure 8 shows the subtropical high being pushed to the east while the low-pressure system moving in from the west starting 2300 HST 21 January 2010. The cold front was approaching the island chain but became stationary to the north of O'ahu. The front never reached O'ahu and moved to the east while remaining north of the island chain. A second cold front moved closer to the island chain 24 January. This cold front passed O'ahu around 0200 HST 27 January. The stalled front to the north of the island along

**Fig. 6** ERA-Interim reanalysis data from 2 February 2010 showing **a** mean sea level (MSL) pressure and **b** geopotential height at 250 mb for the short duration pre-cold front event

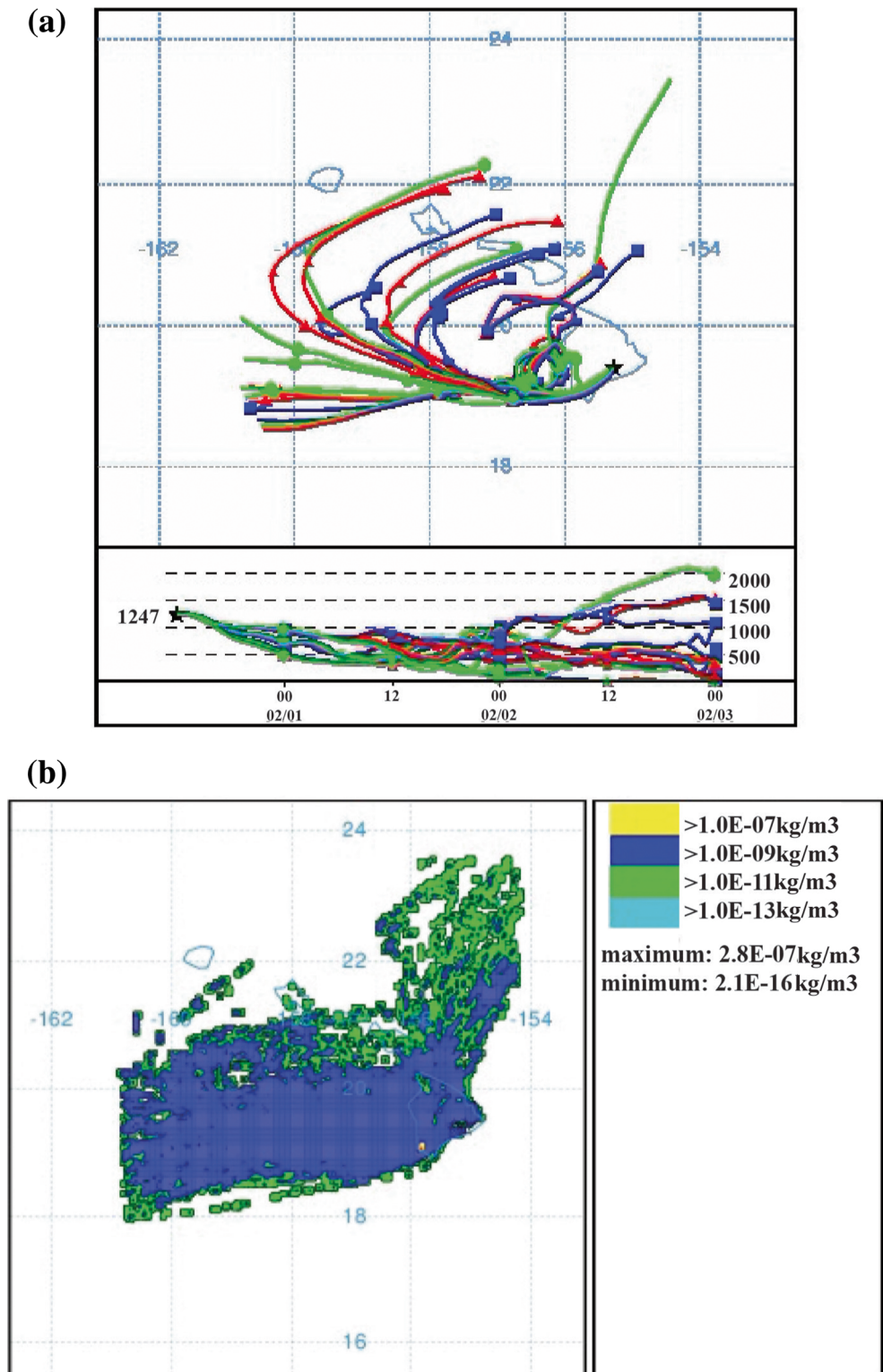


with a second front moving in allowed for a relatively high level of  $PM_{2.5}$  to accumulate and remain over O'ahu for four full days (Fig. 5b).

The ensemble trajectory plot and concentration plots from the HYSPLIT model are found in Fig. 9. In the trajectory plot (Fig. 9a), the wind was initially coming from the

northeast and carrying the plume to the southern tip of Big Island. The winds then turned towards southeasterly and then southwesterly. This time, the winds blew from the south much longer than that in the previous event and turned northwesterly on 23 January. All the members showed a similar trajectory path. Both the cold front cases

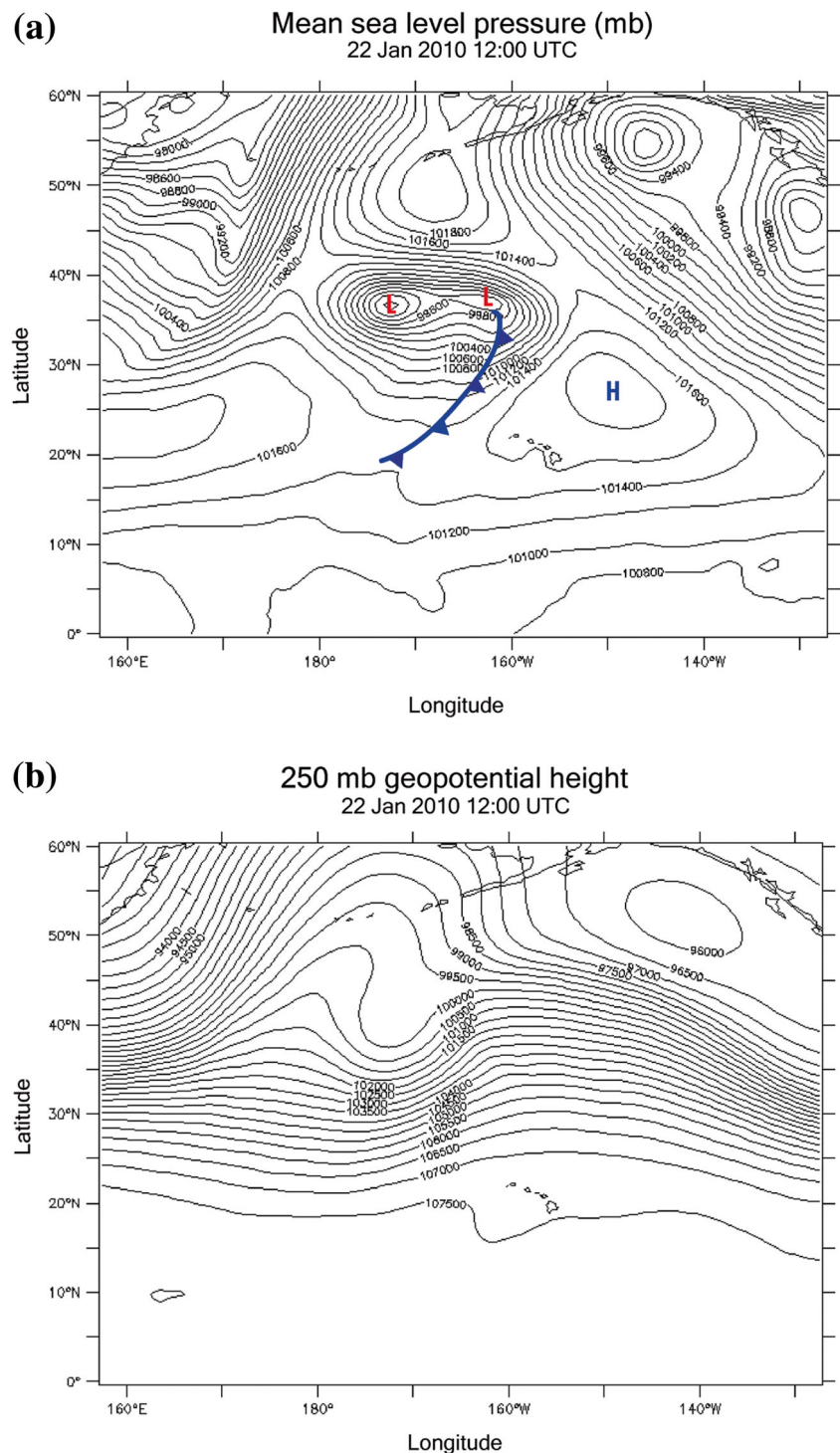
**Fig. 7** HYSPLIT model **a** ensemble trajectory with 27 members and **b** 72-h concentration plot of  $\text{SO}_4$  for the pre-cold front case on 2 February 2010. Both simulations started on 31 January at 1200 UTC



had a similar U-shaped pattern in the trajectory plots. The trajectories start off from the same height but on 22 January 0200 HST, they become more dispersed ranging in height from 0 to 1500 m (Fig. 9a, bottom). Figure 9b shows a

much higher concentration than the previous event, covering the entire island chain and surrounding waters. The event mean value for the long duration case was  $21 \mu\text{g}/\text{m}^3$  per day.

**Fig. 8** The ERA-Interim reanalysis from 22 January 2010 showing **a** MSL pressure and **b** geopotential height at 250 mb for the long duration pre-cold front event

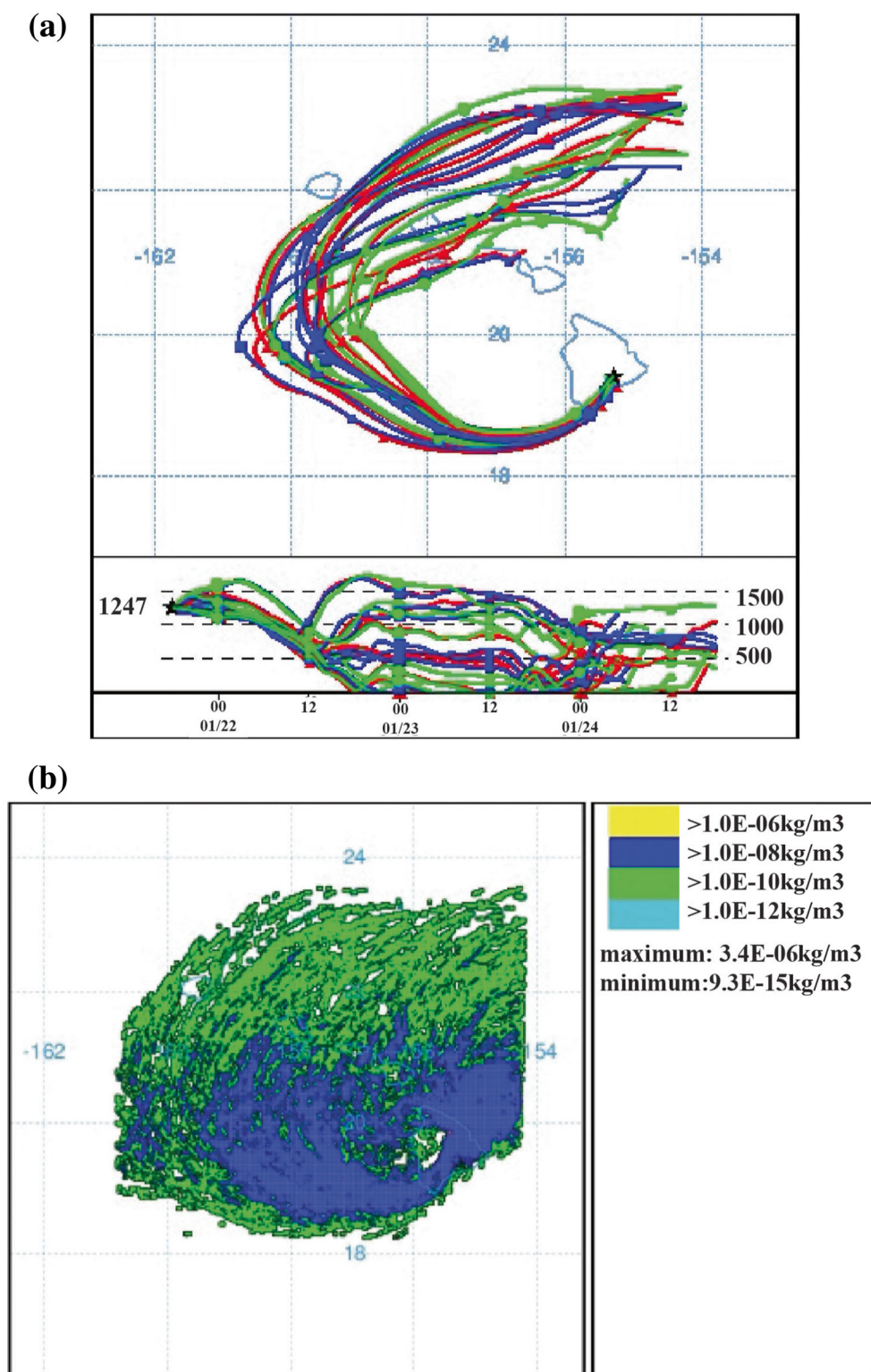


### 3. A Kona low event

The third case was a Kona low from 2 to 3 May 2010. The  $PM_{2.5}$  values started to increase on 1600 HST 2 May and peaked 2000 HST ( $\sim 23 \mu\text{g}/\text{m}^3$ ). The levels stayed high the next day between 8 and  $18 \mu\text{g}/\text{m}^3$  (Fig. 5c).

The reanalysis data for (a) MSL, (b) 850-hPa, (c) 500-hPa, and (d) 250-hPa from 0200 HST 2 May are shown in Fig. 10. The geopotential height at 250-hPa (Fig. 11d) shows the cut-off low from the higher latitude westerlies, and Fig. 10a–c shows how the circulation extended downwards to the surface. Figure 10a has the subtropical high to the

**Fig. 9** HYSPLIT model **a** ensemble trajectory with 27 members and **b** 72-h concentration plot of  $\text{SO}_4$  for the pre-cold front case on 22–24 January 2010. Both simulations started on 21 January at 1800 UTC



northeast of the state, and the surface low to the north-northwest. The circulation at the surface was present for more than 24 h, and the circulation was evident at all levels. Synoptic maps (not shown) had the subtropical high pushed to the east and a low-pressure center with a

stationary front extending from the north of the islands to the mainland USA. The subtropical high and the low-pressure system further deepened and moved slightly northwest. The Kona low eventually dissipated while moving north on 4 May.

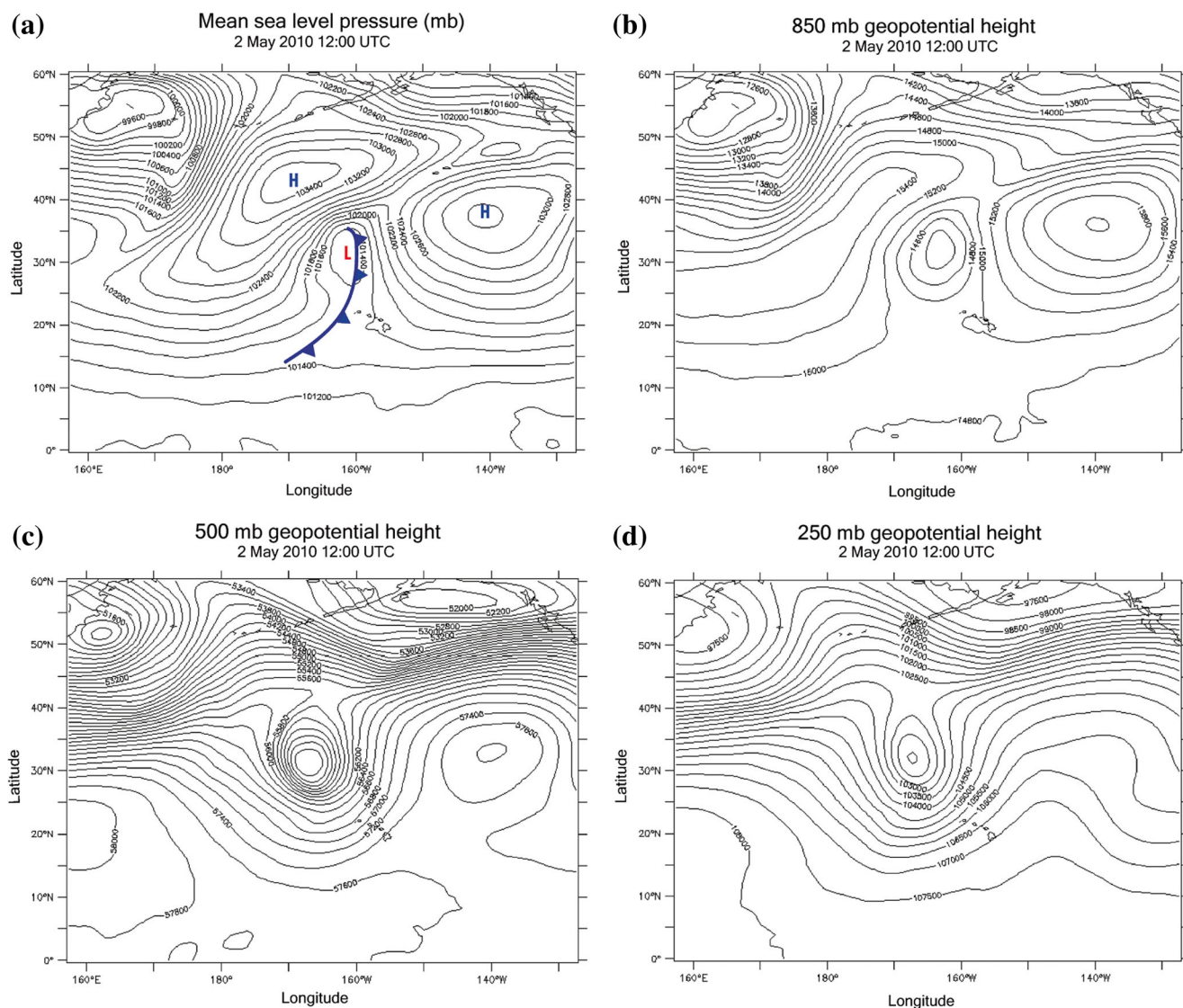


**Fig. 10** The ERA-Interim reanalysis from 2 May 2010 showing **a** MSL pressure, and geopotential height at **b** 850 mb, **c** 500 mb, and **d** 250 mb for the Kona low event

One noteworthy feature about the Kona low is that the location is very important for vog to reach O'ahu. Not all Kona lows bring vog to O'ahu. Only the Kona lows that are located in a favorable location similar to the case presented in Fig. 11, which is to the northwest of the Hawaiian Islands, yields southerly flow.

The ensemble trajectory plot shows that most of the ensemble trajectories traveled a curved path towards the northwest (Fig. 11a). Initially, the winds were out of the northeast, then southeast and eventually from the south. Some of the members got caught in the Big Island wake. Most of the trajectories stay at the same height while slowly decreasing in height throughout their life cycle, except for a few that ascends after 5 May 0200 HST (Fig. 11a, bottom). Figure 11b shows that the plume followed the same curved northwestward track

covering the entire island chain except for the eastern tip of the Big Island. This pattern was different compared to the two prefrontal cases, where the vog plume followed a U-shaped path. In this case, the vog plume went over the islands with the highest concentrations, labeled as dark blue, along the Kona Coast of the Big Island, Maui, and O'ahu. The event mean for the Kona low event was  $17 \mu\text{g}/\text{m}^3$  per day.

#### 4. An upper-level disturbance event

The fourth case was an upper-level disturbance beginning 22 May 2013 with elevated  $\text{PM}_{2.5}$  values for 2 days. The values were high from 1000 to 1700 HST 22 May ranging from 11 to  $22 \mu\text{g}/\text{m}^3$  and high the next day 23 May with values of 6– $26 \mu\text{g}/\text{m}^3$  (Fig. 5d).

**Fig. 11** HYSPLIT model **a** ensemble trajectory with 27 members, and **b** 72-h concentration plot of  $\text{SO}_4$  for the Kona low on 2 February 2010. Both simulations started on 1 May at 1200 UTC

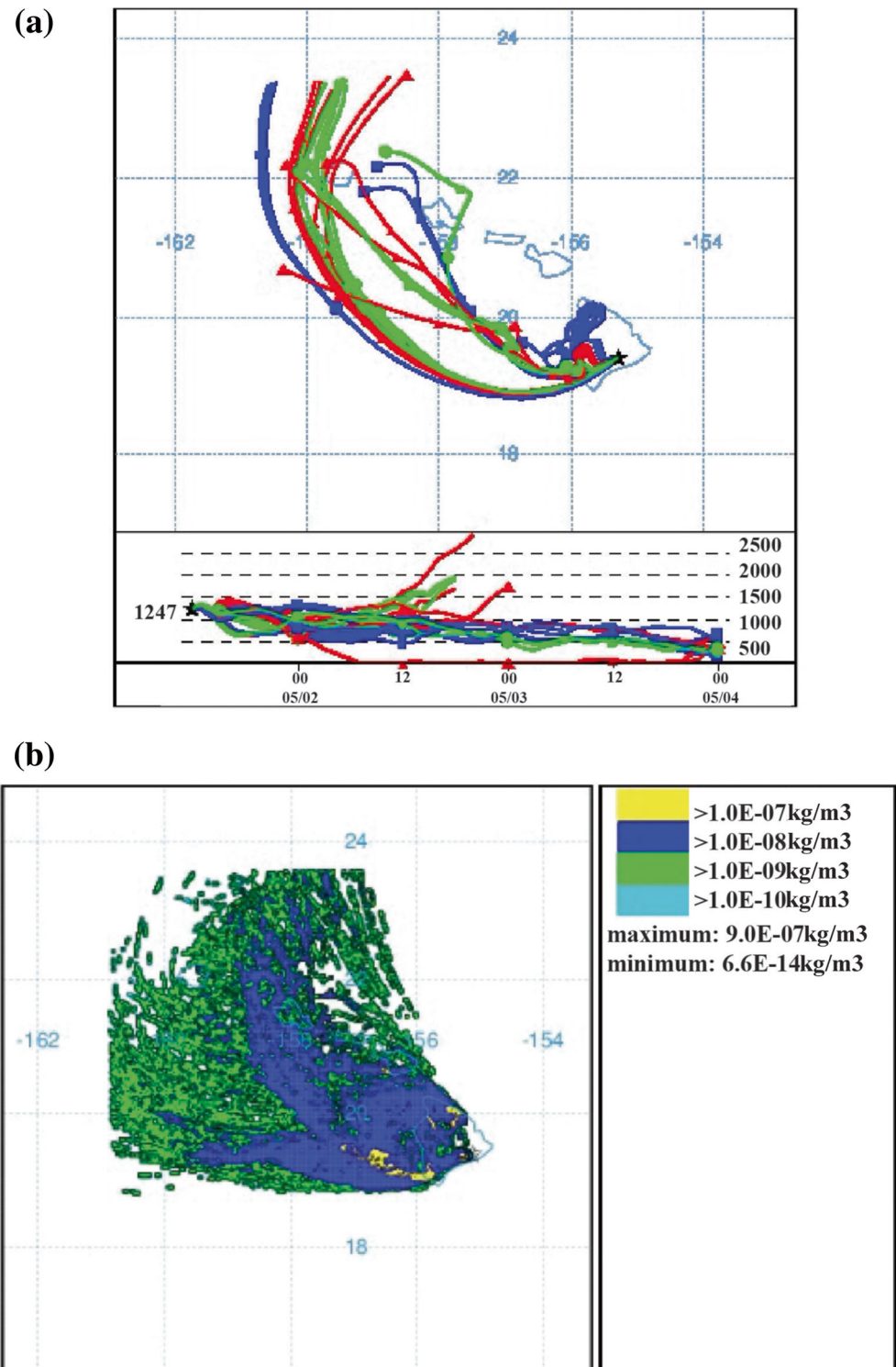
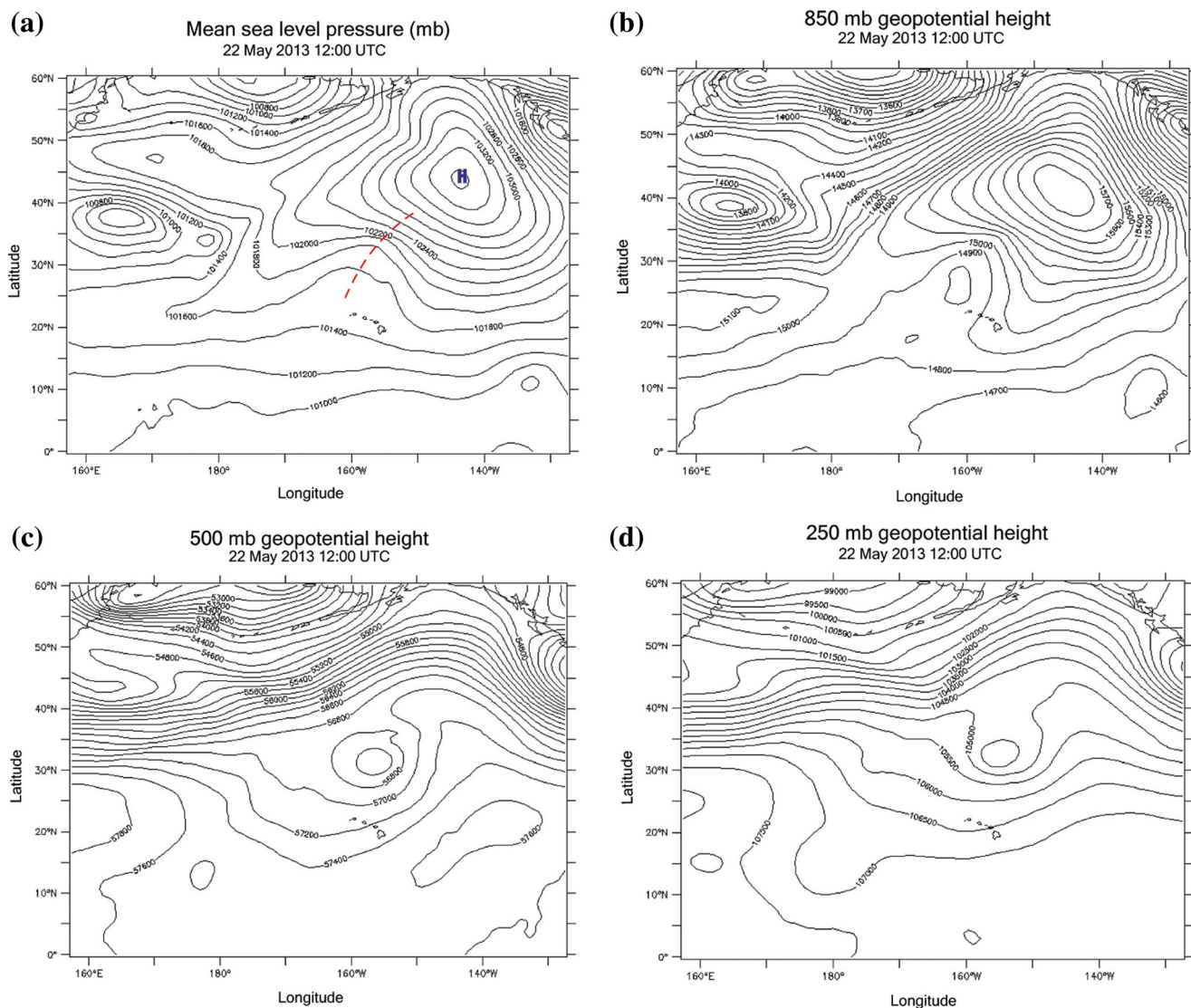


Figure 12 shows the reanalysis data from 0200 HST May 22 displaying the broad subtropical high to the northeast of the state (Fig. 12a). This large-scale weather pattern would normally bring trade winds to the island chain; however, because of an inverted surface trough located near the islands,

the winds had a southerly component. The inverted surface trough was a result of an upper-level low that is clearly seen in the 250-hPa and down to the 850-hPa level (Fig. 12b–d). The trough was also observed in the synoptic map (not shown), from 0200 HST 21 May. Twenty-four hours later, the inverted



**Fig. 12** The ERA-Interim reanalysis from 22 May 2013 showing **a** MSL pressure and geopotential height at **b** 850 mb, **c** 500 mb, and **d** 250 mb for the upper-level disturbance event

trough did start to weaken but still had the winds from the southeast, becoming slightly more pronounced on 24 May and eventually disappearing.

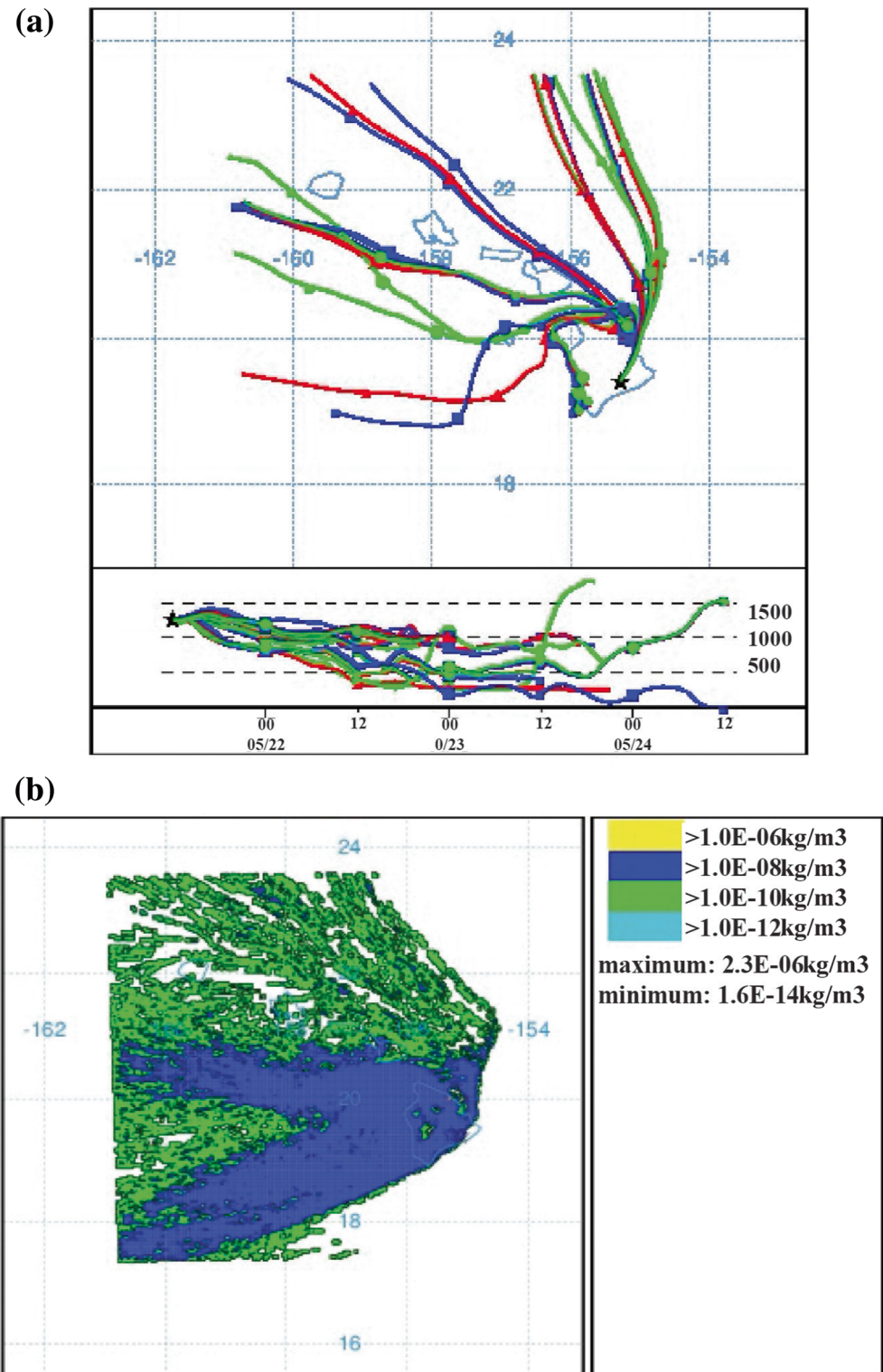
The trajectory plot has a wide range of possible paths with trajectories heading north, northwest, and towards west (Fig. 13a). Four of the trajectories end up along the Kona Coast. Most of the trajectories leave the domain at 1200 UTC 23 May, and only three trajectories stay in the domain slightly longer. This happened because the winds were stronger during this event, causing the released particles to leave the domain faster compared to the other events. This is also evident in the height plot which shows that most of the trajectories slowly decrease in height with time until they disappear from the plot (Fig. 13a, bottom). Two of the trajectories ascend after 22 May. The concentration plot shows that the southerly winds initially brought the vog plume towards the north

(Fig. 13b). The winds then slowly continue to shift and at the end of the concentration plot, the vog plume is heading towards the west. The highest concentrations are mainly over the Big Island and the area to the west of the island chain with lower values over the smaller islands (Fig. 13b). The event mean for the upper-level disturbance case was  $19 \mu\text{g}/\text{m}^3$  per day.

## Conclusion and discussion

The DOH  $\text{PM}_{2.5}$  measurements from Honolulu were used to identify 101 vog days over a 5-year and 9-month period. Unfortunately, we could only use one of four stations on O'ahu due to background pollution. Understanding this limitation, we identified that vog days represent 4.8% of the period

**Fig. 13** HYSPLIT model **a** ensemble trajectory with 27 members and **b** 72-h concentration plot of  $\text{SO}_4$  for the upper-level disturbance on 22–23 May 2013. Both simulations started on 21 May at 1200 UTC



from April 2009 to 2014. ERA-Interim data were examined along with ocean products from SRRS to determine the large-scale weather patterns associated with each vog day. Results showed that the 101 vog days were associated with 57 vog events lasting up to 4 days. Vog does not reach O'ahu during regular trade wind days. Instead, all the vog events occurred

under the influence of one of three different synoptic-scale disturbances. These are (1) pre-cold fronts, (2) Kona lows, and (3) upper-level disturbances. The pre-cold fronts are further divided into short- and long-duration events, resulting in a total of four case studies. It is rare to experience vog events during summertime, and most of the events occurred from

October through May. During the vog events, the PM<sub>2.5</sub> measurements had an oscillating behavior and were not continually high throughout the event.

The next objective was to dynamically downscale the ERA-Interim reanalysis data from four case studies and to simulate them in HYSPLIT to demonstrate how the vog plume behaved in each type of synoptic pattern. Downscaling from ~ 80 to 10 km to ~ 3 km to run the HYSPLIT model will not capture all the nuances of airflow through the archipelago. Also, day to day variations in the output of SO<sub>2</sub> from the volcano were not known. We have also assumed an instantaneous conversion of SO<sub>2</sub> to SO<sub>4</sub> particulate. How SO<sub>4</sub> particulates interact with clouds and rain is only crudely approximated in the HYSPLIT model. However, with these limitations in mind, the two prefrontal cases showed a U-shaped ensemble trajectory path from the Big Island to O'ahu. The Kona low to the north of the Hawaiian Island allowed the vog plume to be carried across the state by the southeasterly winds. The upper-level disturbance altered the trade-wind flow to create a trough at the surface that brought vog from the vents to O'ahu.

The majority of the event types were prefrontal, which were responsible for 65% of the total number, 30% were upper-level disturbances, and only 5% were due to Kona lows. The pre-cold fronts with a longer duration bring in the highest levels of vog to O'ahu. As seen in this study, weak southerly winds that persist for a long time will lead to an accumulation of vog over parts of the island chain. The longer duration event case had a mean value of 21 µg/m<sup>3</sup>. The mean and median value for the 18 events found of the long-duration type was 18 µg/m<sup>3</sup>, and this synoptic pattern caused the worst PM<sub>2.5</sub> pollution. The annual number of Kona lows varies from year to year; however, the center of the low needs to pass through a region north of Hawai'i in order for the vog to reach O'ahu. During the Kona low case study, the vog plume was transported across the entire island chain from the southeast towards the northwest with a slight arc in the trajectories. Upper-level disturbances can occur any time of the year but during this period, vog reached O'ahu only during wintertime. For an upper-level disturbance to cause a vog occurrence on O'ahu, it must alter the flow in the trade wind layer.

A desirable condition would be the establishment of more vog monitoring stations on the island of O'ahu, and eventually a longer period of PM<sub>2.5</sub> measurements. New stations should be placed away from industrial areas and highways and be placed from the westside of O'ahu to the southeast such as Hawai'i Kai. More stations would allow for improved spatial coverage during vog events.

**Acknowledgements** The authors would like to thank Dr. Andre Marquez, Dr. Mathew Stiller-Reeve, Dr. John Porter, and Chris Holloway for useful discussions and guidance during the course of this work. Chris Ostrander of UH SOEST was helpful in the initial phase of

this study. We also express our appreciation to Andre Pattantyus as an official reviewer for careful reading and many good suggestions which led to a significant improvement of the presentation of this paper. Kristine Tofte was funded by the Joint Institute of Marine and Atmospheric Research (JIMAR) of the University of Hawai'i for the first 2 years, and by the Honolulu Board of Water Supply C13548001 (Pao-Shin Chu) and the National Science Foundation AGS-1042680 (Gary Barnes) for the last 5 months.

The DOH PM<sub>2.5</sub> data is available upon request. The ERA-Interim data is available through <http://www.ecmwf.int/en/research/climate-reanalysis/era-interim>, and the NOAA ocean analysis is retrieved from <http://nomads.ncdc.noaa.gov>. Version 3.5 of the Advanced Research WRF (WRFV3.5) was downloaded and used through the Computational and Information Systems Laboratory (CISL), which is run by the National Center for Atmospheric Research. More specifically, the Yellowstone system was used, which is a high-performance computing resource. HYSPLIT is available through <http://ready.arl.noaa.gov/HYSPLIT.php>.

## References

- Businger S, Huff R, Pattantyus A, Horton K, Sutton AJ, Elias T, Cherubini T (2015) Observing and forecasting vog dispersion from Kilauea volcano, Hawai'i. *Bulletin Am Meteor Soc* 96(10):1667–1686
- Caruso SJ, Businger S (2006) Subtropical cyclogenesis over the central North Pacific. *Weather Forecast* 20:193–205
- Chu PS, Wang J (1997) Tropical cyclone occurrences in the vicinity of Hawai'i: are the differences between El Niño and non-El Niño years significant? *J Clim* 10:2683–2689
- Chu PS, Nash AJ, Porter FY (1993) Diagnostic studies of two contrasting rainfall episodes in Hawai'i: dry 1981 and wet 1982. *J Clim* 6:1457–1452
- Dee DP, Uppala SM, Simmons AJ, Berrisford P, Poli P, Kobayashi S, Andrae U, Balmaseda MA, Balsamo G, Bauer P, Bechtold P, Beljaars ACM, van de Berg L, Bidlot J, Bormann N, Delsol C, Dragani R, Fuentes M, Geer AJ, Haimberger L, Healy SB, Hersbach H, Hólm EV, Isaksen I, Kållberg P, Köhler M, Matricardi M, McNally AP, Monge-Sanz BM, Morcrette JJ, Park BK, Peubey C, de Rosnay P, Tavolato C, Thépaut JN, Vitart F (2011) The ERA-interim reanalysis: configuration and performance of the data assimilation system. *QJR Meteorol Soc* 137:553–597
- Draxler RR, Hess GD (1998) An overview of the HYSPLIT\_4 modelling system for trajectories, dispersion, and deposition. *Aust Met Mag* 47:295–308
- Durand M, Grattan J (2001) Effects of volcanic air pollution on health. *Lancet* 357(9251):164
- Fann N, Rislely D (2013) The public health context for PM 2.5 and ozone air quality trends. *Air Qual Atmos Health* 6:1–11
- Fleming ZL, Monks PS, Manning AJ (2012) Review: untangling the influence of air-mass history in interpreting observed atmospheric composition. *Atmos Res* 104:1–39
- Garza J, Chu PS, Norton C, Schroeder TA (2012) Changes of the prevailing trade winds over the islands of Hawai'i and the North Pacific. *J Geophys Res* 117:D11109. doi:10.1029/2011JD016888
- Hodges KI, Lee RW, Bengtsson L (2011) A comparison of extratropical cyclones in recent reanalyses ERA-interim, NASA MERRA, NCEP CFSR, and JRA-25. *J Clim* 24:4888–4960
- Kelley WE, Mock DR (1982) A diagnostic study of upper tropospheric cold lows over the western North Pacific. *Bulletin Am Meteor Soc* 110:71–480

- Kodama K, Barnes GM (1997) Heavy Rain Events over the South-Facing Slopes of Hawaii: Attendant Conditions. *Weather Forecast* 12(2): 347–367
- Li Y, Henze DK, Jack D, Kinney PL (2016) The influence of air quality model resolution on health impact assessment for fine particulate matter and its components. *Air Qual Atmos Health* 9(1):51
- Longo BM (2009) The Kīlauea volcano adult health study. *Nurs Res* 58: 23–31
- Longo BM (2013) Adverse health effects associated with increased activity at Kīlauea Volcano: A repeated population-based survey. *ISRN Public Health* 2013. <https://doi.org/10.1155/2013/475962>
- Morrison I, Businger S (2000) Synoptic structure and evolution of a Kona low. *Wea Forecasting* 16:81–98
- O'Connor CF, Chu PS, Hsu PC, Kodama K (2015) Variability of Hawaiian winter rainfall during La Nina events since 1956. *J Clim* 28:7809–7832
- Otkin JA, Martin JE (2004) A synoptic climatology of the subtropical Kona storm. *Mon Weather Rev* 132:1502–1517
- Porter JN, Horton KA, Mouginiis-Mark PJ, Lienert B, Sharma SK., Lau E, Oppenheimer C (2002) Sun photometer and lidar measurements of the plume from the Hawai'i Kīlauea Volcano Pu'u O'o vent: Aerosol flux and SO<sub>2</sub> lifetime. *Geophysical Research Letters* 29(16)
- Rutledge GK, Alpert J, Ebisuzaki W (2006) NOMADS: a climate and weather model archive at the National Oceanic and Atmospheric Administration. *Bull Am Meteorol Soc* 87:327–341
- Sadler JC (1975) The tropical upper tropospheric trough as a second source of typhoons and a primary source of trade wind disturbances. Hawai'i Institute of Geophysics Rep.-67–12, pp 44 [Available from HIG, 2525 Correa Rd., Honolulu, HI 96822]
- Simpson RH (1952) Evolution of the kona storm: a subtropical cyclone. *J Meteorol* 9:24–35
- Skamarock WC, Klemp JB, Dudhia J, Gill DO, Barker DM, Wang W, Powers JG (2008) A description of the Advanced Research WRF Version 3, NCAR technical note, Mesoscale and Microscale Meteorology Division. National Center for Atmospheric Research, Boulder, Colorado, USA
- State of Hawai'i Department of Health (2014) Annual summary 2013. Retrieved from <http://health.hawaii.gov/cab>
- Sutton J, Elias T, Hendley WH, Stauffer PH (2000) USGS Fact Sheet 169–97, version 1.1
- Tu CC, Chen YL (2011) Favorable conditions for the development of a heavy rainfall event over O'ahu during the 2006 wet period. *Weather Forecast* 26:280–300
- Worthley LE (1967) Synoptic climatology of Hawai'i. *Weather phenomena in Hawai'i, part I*. Hawai'i Institute of Geophysics Rep 67-9:1–40